Fragility functions for tall URM buildings around early 20th century in Lisbon.
Part 2: application to different classes of buildings

Ana G. Simões[1], Rita Bento[1*], Sergio Lagomarsino[2], Serena Cattari[2], Paulo B. Lourenço[3]

[1]CERIS, Instituto Superior Técnico, Universidade de Lisboa, Lisbon (Portugal)

[2]DICCA, Università Degli Studi di Genova, Genoa (Italy)

[3]ISISE, Universidade do Minho, Campus de Azurém, Guimarães (Portugal)

*Corresponding Author: Address: Av. Rovisco Pais, 1, 1049-001 Lisboa, Portugal;

Email: rita.bento@tecnico.ulisboa.pt; Tel: +351 218 418 210

Abstract

This article describes the application of the procedure for the derivation of fragility functions presented in the companion article entitled *Fragility functions for tall URM buildings around early 20th century in Lisbon. Part 1: methodology and application at building level.* The procedure, based on the execution of non-linear analyses, was developed to be applied to unreinforced masonry buildings considering both the in-plane and out-of-plane response. Different sources of uncertainty, both epistemic and aleatory, affecting the behaviour of these unreinforced masonry buildings are discussed and treated with a probabilistic procedure. The fragility curves determined for the different classes of buildings are compared and then combined to define the final fragility curves for these unreinforced masonry buildings. The results put in evidence the high seismic vulnerability of these buildings and the urgent need for the structural intervention and for the design of retrofitting measures in order to reduce potential losses due to future earthquakes.

Keywords

Unreinforced Masonry Buildings; Seismic Vulnerability; Fragility Functions; Non-Linear Static Analysis; Non-Linear Kinematic Analysis; Non-Linear Dynamic Analysis

1

1. Introduction

Seismic vulnerability addresses the susceptibility to suffer damage or loss due to an earthquake. It can be defined using fragility functions, providing the probability of reaching or exceeding a specified limit state as a function of a selected seismic intensity measure. The main objective of this work is to apply, to different classes of unreinforced masonry (URM) buildings around early 20th century in Lisbon, the procedure proposed for the derivation of fragility functions in the companion article (Part 1, Simões et al., 2019a). This procedure is based on non-linear analyses and takes into account different sources of uncertainties that influence the seismic performance.

In Simões et al. (2019a) the main steps of the procedure are presented. Basically, it comprehends the generation of fragility functions for the in-plane and out-of-plane response following different criteria and methods of analyses. The in-plane response refers to the global (box-type) behaviour controlled by the in-plane capacity of walls and stiffness of horizontal diaphragms. The out-of-plane response refers to the activation of local mechanisms, typically consisting on the overturning of parts of the building insufficiently connected to the rest of the structure. The fragility curves individually obtained for the in-plane and out-of-plane response are after combined in order to define a single fragility curve. The capacity curves are evaluated, for the in-plane response, through non-linear static (pushover) analyses, and, for the out-of-plane response, through non-linear kinematic analyses. The intensity measure that produces the attainment of the limit state is obtained from the application of the Capacity-Spectrum Method with overdamped spectrum, as proposed in (Lagomarsino and Cattari, 2015). The method comprises the comparison between the displacement capacity of the structure for a limit state threshold and the seismic demand, in an acceleration-displacement coordinates system (refer to §2 from Part 1, Simões et al., 2019a). The final dispersion of the fragility curves results from the contribution of both aleatory and epistemic uncertainties on the structural capacity and the aleatory uncertainty on the seismic demand.

This article addresses the application of the procedure proposed in Simões et al. (2019a) to one of the most vulnerable unreinforced masonry buildings constructed in the early 20th century in Lisbon, examining a typical prototype building with five storeys high. Considering that these buildings are located in the middle or in the end of a row of buildings, a group of three equal buildings is considered to evaluate the effect of the aggregate in the seismic behaviour.

Then, for this type of buildings, proper classes are defined (Simões et al., 2018; Simões, 2018) as a function of their similarity in structural details, material and seismic response. The features that mostly affect the seismic performance are identified depending on the available data and characteristics of the masonry buildings under investigation. In this work, these features are considered as epistemic uncertainties (related to the incomplete knowledge) and are treated by the logic-tree approach. Moreover, effective strategies to reduce the number of buildings classes and, thus limit the computational effort required in executing the non-linear static analyses, are discussed. Finally, the fragility curves determined for the different classes of buildings, selected as the "minima" required to obtain a reliable description of the behaviour of the structural typology under examination, are compared and the final fragility curves for these unreinforced masonry buildings are provided.

2. The URM "gaioleiro" buildings

2.1. Identification of classes of buildings

The development of vulnerability models at territorial scale firstly requires the identification of classes of buildings. This is supported on the idea that buildings with similar architectural and structural features and located in similar geotechnical conditions are expected to have a similar seismic performance. Thus, the features that mostly affect the seismic performance must be singled out depending on the characteristics of the building stock. As mentioned in §1, different classes of buildings have been identified in previous works for the URM "gaioleiro" buildings in Lisbon (Simões et a.l, 2018; Simões, 2018). The different classes of buildings account for geometry variations at the ground floor level, constructive details and materials attributed to the different walls. All these features are considered as epistemic uncertainties (related to the incomplete knowledge) and are treated by the logic-tree approach. A subjective probability is attributed to each feature based on the information available in the literature and on a detailed survey to a block of URM buildings in "Avenidas Novas" (Simões et al., 2016). This aims to define different prototypes representative of the URM buildings constructed in Lisbon in the early 20th century, starting from the prototype building defined in (Simões et al., 2019a).

Geometry: ground floor configuration

The ground floor level may be used as housing or as shop, implying a different layout of openings as exemplified in Figure 1. Taking into account the reference block of buildings that has been surveyed, the ground floor of 33% of the buildings is used as housing and 67% is used for shop. The regular floors are used as housing in both cases.
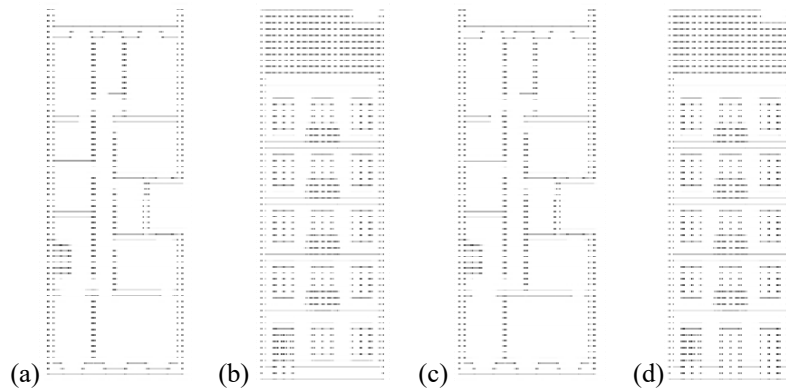
Figure 1 – Prototype building as housing (a) plan view and (b) street view, and as shop (c) plan view and (d) street view

Constructive Details

The typical building is located in the middle or in the end of a row of buildings; no isolated configuration can occur. According to the 1867 law (Código Civil, Decreto 01/07/1867, cited in (Appleton, 2005)) the side walls could be shared between adjacent buildings. The decision may depend on the time of construction and on the dimension of the lot. In the reference block of buildings, 33% of the buildings have shared side walls and 67% have independent side walls. In order to take into account the effect of the adjacent buildings (i) and the possibility that the side walls are shared or independent between buildings (ii), it is proposed to replicate the prototype building and define a group of three buildings as case of study, as shown in Figure 2.
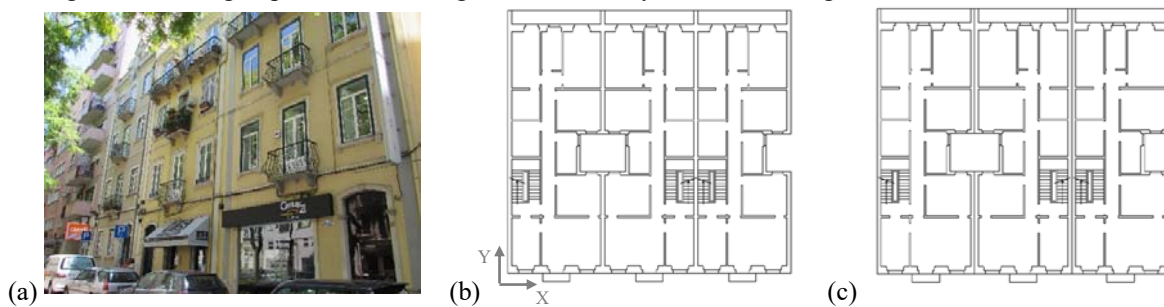

Figure 2 – URM buildings: (a) view from the block of buildings in "Avenidas Novas", (b) group of buildings with shared side walls and (c) group of buildings with independent side walls

Materials

One of the main features affecting the seismic performance of URM buildings are the materials and mechanical properties of the materials used in the construction of the walls. During this period of construction in Lisbon, the URM buildings may include rubble stone masonry walls, clay brick (solid or hollow units) masonry walls and timber walls. However, there is few information in the buildings' process (in Arquivo Municipal de Lisboa, AML, http://arquivomunicipal.cm-lisboa.pt/) about the material employed in the different walls. Due to this limitation, all possibilities are examined and a subjective probability is attributed in order to quantify the representativeness of the option within the building stock.

Exterior walls were constructed in rubble stone masonry on the street and rear façade walls and clay brick masonry on the side walls. Brick units may be: i) solid in all floors or ii) solid in the lower floors and hollow in the upper floors. The Building Regulation from 1930 (RGEUL, 1930) recommended to use hollow bricks only in the last two floors of the side walls. Considering that this regulation was published in the end of the construction age of these buildings, a lower probability is attributed to this option. Therefore, it may be assumed that the side walls of 70% of the buildings are made of solid clay brick masonry, while the remaining 30% are made of solid clay brick masonry in the first three floors and hollow clay brick masonry in the last two floors.

In what concerns interior walls, it is estimated that the main walls are made of solid clay brick masonry in 50% of the buildings while they are made of solid clay brick masonry in the ground floor and hollow clay brick masonry in the other floors in 50% of the buildings. However, there are records of buildings in which most of the interior walls are made with timber structure. In order to consider also this option, it is proposed to assume that in 20% of the buildings the main interior walls are made of timber (but limiting them to the last floor of the buildings, as indicated in (RGEUL, 1930)) and to reduce the previous probabilities associated to clay brick masonry to 40/40. As to the partition walls, it is estimated that in 50% of the buildings these are made of hollow clay brick masonry, while in 50% of the buildings these are made of timber structure.

3

2.2. Logic-Tree Approach: epistemic uncertainties

From the data illustrated in §2.1, the main variations identified for the tall URM "gaioleiro" buildings are summarized as:

1. Ground floor configuration: use of the building as i) housing (H) or as ii) shop (S).
2. Side walls solution: i) side walls shared between adjacent buildings (S) or ii) independent (I).
3. Side walls material: i) solid clay brick masonry (S) or ii) solid clay brick masonry in the first two floors and hollow clay brick masonry in the last three floors (SH).
4. Main interior walls material: i) solid clay brick masonry (S), ii) solid clay brick masonry in the first two floors and hollow clay brick masonry in the last three floors (SH), or iii) solid clay brick masonry in the first two floors, hollow clay brick masonry in the medium floors and timber walls on the last floor (T).
5. Partition walls material: i) hollow brick masonry (H) or ii) timber walls (T).

These variations are considered as epistemic uncertainties and are organized in a logic-tree. This allows to define different classes representative of the URM buildings constructed in Lisbon in the early 20th century. Each node of the tree represents a specific feature of the buildings and each branch represents an alternative option associated to that feature. Finally, the end of a branch of the tree represents a class of buildings with specific features, identified by an acronym (starting from the capital letters in the numbers above). The probability attributed to the class of buildings is determined by multiplying the probability of all the component branches of the tree. The logic-tree proposed for the tall URM "gaioleiro" buildings is presented in Figure 3, comprising a total of 32 building classes (identified as group A).
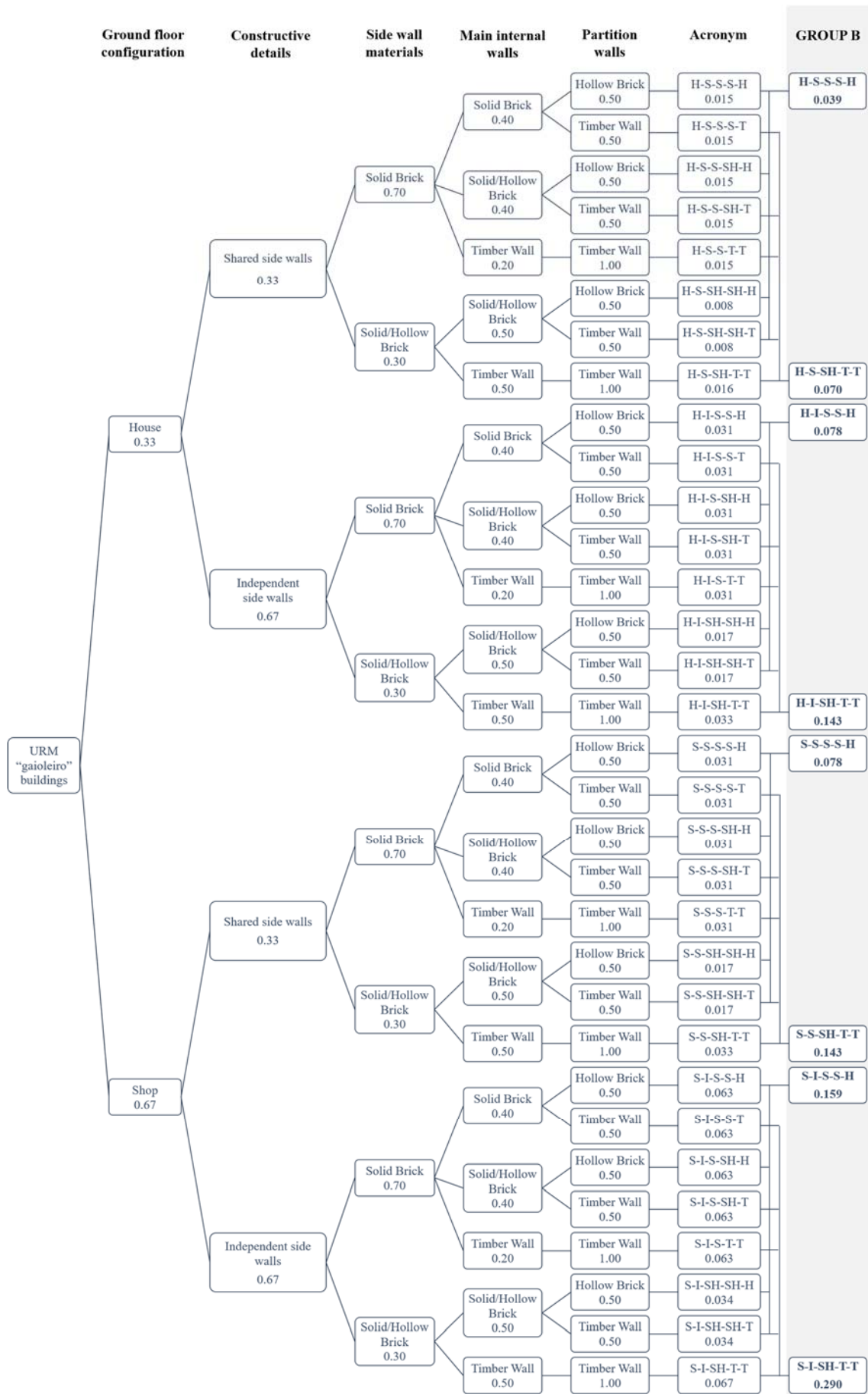
Figure 3 – Logic-tree for the tall URM "gaioleiro" buildings

Root: URM "gaioleiro" buildings

Ground floor configuration	Constructive details	Side wall materials	Main internal walls	Partition walls	Acronym		GROUP B
House 0.33	Shared side walls 0.33	Solid Brick 0.70	Solid Brick 0.40	Hollow Brick 0.50	H-S-S-S-H	0.015	H-S-S-S-H 0.039
				Timber Wall 0.50	H-S-S-S-T	0.015	
			Solid/Hollow Brick 0.40	Hollow Brick 0.50	H-S-S-SH-H	0.015	
				Timber Wall 0.50	H-S-S-SH-T	0.015	
			Timber Wall 0.20	Timber Wall 1.00	H-S-S-T-T	0.015	
		Solid/Hollow Brick 0.30	Solid/Hollow Brick 0.50	Hollow Brick 0.50	H-S-SH-SH-H	0.008	
				Timber Wall 0.50	H-S-SH-SH-T	0.008	
			Timber Wall 0.50	Timber Wall 1.00	H-S-SH-T-T	0.016	H-S-SH-T-T 0.070
	Independent side walls 0.67	Solid Brick 0.70	Solid Brick 0.40	Hollow Brick 0.50	H-I-S-S-H	0.031	H-I-S-S-H 0.078
				Timber Wall 0.50	H-I-S-S-T	0.031	
			Solid/Hollow Brick 0.40	Hollow Brick 0.50	H-I-S-SH-H	0.031	
				Timber Wall 0.50	H-I-S-SH-T	0.031	
			Timber Wall 0.20	Timber Wall 1.00	H-I-S-T-T	0.031	
		Solid/Hollow Brick 0.30	Solid/Hollow Brick 0.50	Hollow Brick 0.50	H-I-SH-SH-H	0.017	
				Timber Wall 0.50	H-I-SH-SH-T	0.017	
			Timber Wall 0.50	Timber Wall 1.00	H-I-SH-T-T	0.033	H-I-SH-T-T 0.143
Shop 0.67	Shared side walls 0.33	Solid Brick 0.70	Solid Brick 0.40	Hollow Brick 0.50	S-S-S-S-H	0.031	S-S-S-S-H 0.078
				Timber Wall 0.50	S-S-S-S-T	0.031	
			Solid/Hollow Brick 0.40	Hollow Brick 0.50	S-S-S-SH-H	0.031	
				Timber Wall 0.50	S-S-S-SH-T	0.031	
			Timber Wall 0.20	Timber Wall 1.00	S-S-S-T-T	0.031	
		Solid/Hollow Brick 0.30	Solid/Hollow Brick 0.50	Hollow Brick 0.50	S-S-SH-SH-H	0.017	
				Timber Wall 0.50	S-S-SH-SH-T	0.017	
			Timber Wall 0.50	Timber Wall 1.00	S-S-SH-T-T	0.033	S-S-SH-T-T 0.143
	Independent side walls 0.67	Solid Brick 0.70	Solid Brick 0.40	Hollow Brick 0.50	S-I-S-S-H	0.063	S-I-S-S-H 0.159
				Timber Wall 0.50	S-I-S-S-T	0.063	
			Solid/Hollow Brick 0.40	Hollow Brick 0.50	S-I-S-SH-H	0.063	
				Timber Wall 0.50	S-I-S-SH-T	0.063	
			Timber Wall 0.20	Timber Wall 1.00	S-I-S-T-T	0.063	
		Solid/Hollow Brick 0.30	Solid/Hollow Brick 0.50	Hollow Brick 0.50	S-I-SH-SH-H	0.034	
				Timber Wall 0.50	S-I-SH-SH-T	0.034	
			Timber Wall 0.50	Timber Wall 1.00	S-I-SH-T-T	0.067	S-I-SH-T-T 0.290

Figure 3 – Logic-tree for the tall URM "gaioleiro" buildings

3. Strategies to improve the procedure for the derivation of fragility functions for the global behaviour

3.1. Sensitivity analyses to reduce the number of classes of buildings

Non-linear static (pushover) analyses are carried out to the 32 classes of buildings models defined by the epistemic uncertainties (Figure 3) and by the median properties of the aleatory variables identified in the companion article (Simões et al., 2019a). The analyses are performed in Tremuri program (Lagomarsino et al., 2013) considering the two main directions of the group of buildings (X – parallel to the façade walls and Y – parallel to the side walls). At this stage, only the uniform load distribution (proportional to the mass) is considered and applied on the positive direction of the building. In addition, the connections between perpendicular exterior walls are kept by default as good quality, i.e., the aleatory variables from Group 16 (see Table 1 in (Simões et al., 2019a)) related to the properties of the link beams were not considered because these implied additional modifications to the numerical model and would not affect the main conclusions. The objective is to perform a sensitivity analysis and compare the global seismic behaviour of the different classes of buildings.

Figure 4 to Figure 7 plot the pushover curves as the ratio between the base shear force and the weight of the structure (V/W) in function of the average displacement of the roof weighted by the seismic modal mass of all nodes (d). For a matter of simplicity, the 32 models are divided in four groups linked to the first two letters of the acronyms.
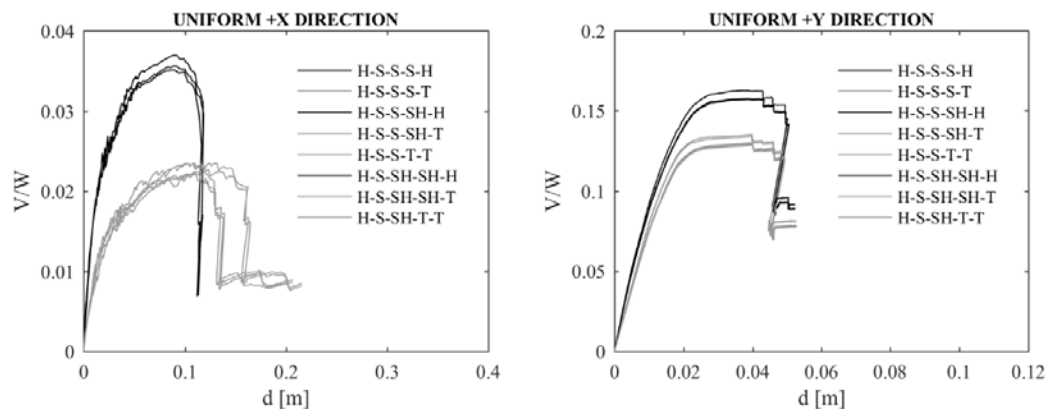
Figure 4 – Pushover curves for the first the group of buildings (H-S): X direction (left) and Y direction (right)
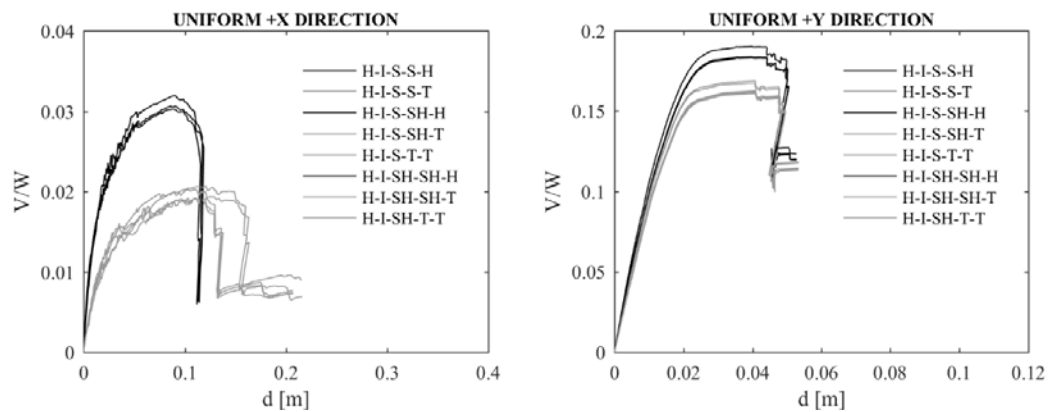
Figure 5 – Pushover curves for the second group of buildings (H-I): X direction (left) and Y direction (right)
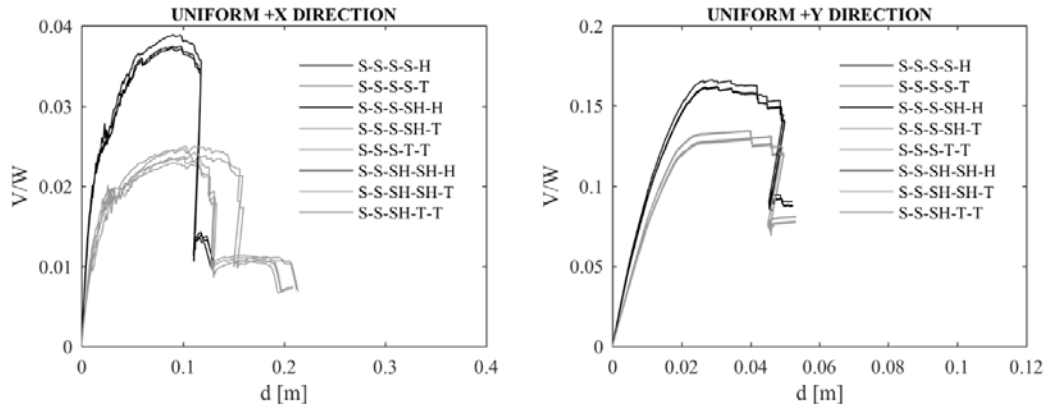
Figure 6 – Pushover curves for the third group of buildings (S-S): X direction (left) and Y direction (right)
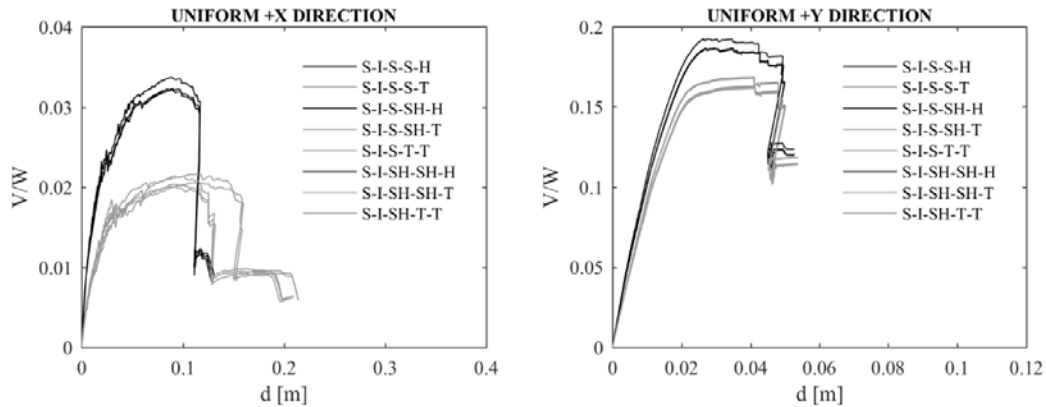
Figure 7 – Pushover curves for the fourth group of buildings (S-I): X direction (left) and Y direction (right)

Within each group, it is evident a similar behaviour between models with and without timber walls (grey vs. black lines) concerning initial stiffness (K), ratio between maximum base shear force and weight (V_{max}/W) and maximum displacement (d_{max}). The variations are higher in the X direction than in the Y direction, but in all cases the Coefficient of Variation (CoV) is lower than 10%. Thus, it is proposed to consider two models from each of the four groups – one with and one without timber walls – and reduce the number classes of buildings from 32 to 8. The selection of the classes is based on the ones with the highest probability. The final probabilities are updated in the logic-tree by summing the contribution of the suppressed models, so that the final probability is equal to 1. The final 8 classes of buildings are presented in the logic-tree from Figure 3 and identified as group B.

The numerical model of the buildings is after modified in order to introduce the link beams on the connection between walls, as explained in (Simões et al., 2019a) – see §3.1- to simulate the effectiveness of the wall-to-wall connection. Figure 8 presents the pushover curves for the 8 final classes of buildings obtained with the application of the uniform load distribution.
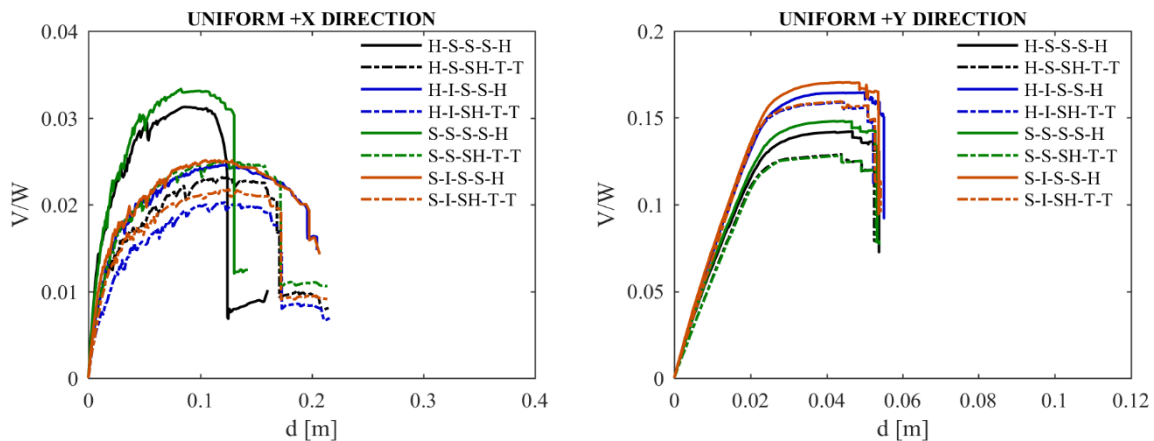
Figure 8 – Pushover curves for the final classes of buildings: X direction (left) and Y direction (right)

The seismic behaviour in the X direction is, in general, characterized by: i) lower stiffness and strength for classes of buildings with timber walls (#-#-SH-T-T) in comparison with the ones without such walls (#-#-S-S-H); ii) lower stiffness and strength for classes of buildings with independent side walls (#-I-#-#-#) in comparison with shared side walls (#-S-#-#-#). This can be explained by the reduction of the flange effect induced by the exterior walls on the perpendicular walls (and the consequent reduction of the forces on the masonry piers from the interior walls). In the Y direction, classes of buildings with shared side walls (#-S-#-#-#) have lower stiffness and strength, due to the lower thickness of the side walls. The use of the ground floor as house (H-#-#-#-#) results on the lower value of the maximum base shear in both directions, as a consequence of the different layout of the prototype building (Figure 2), despite the small differences in contrast with models with shop use (S-#-#-#-#).

3.2. Monte Carlo Simulations: aleatory uncertainties

The dispersion of the fragility curve (β) takes into account also the aleatory variability in the definition of the capacity (β_C). The latter is related to the random/aleatory variables aiming to account for both the uncertainties in the quantification of specific parameters and the intrinsic variations between buildings.

In this work, a total of 50 aleatory variables are considered for the analysis of the global behaviour (Simões et al., 2019a). The Monte Carlo Method (Rubinstein, 2011) is used to define possible outcome values for each aleatory variables. The number of simulations is defined in order to have a sufficient number of results to reach good estimation of the parameters that define fragility functions for the building class. Following this assumption, 1000 Monte Carlo simulations are considered to sample each of aleatory variables starting from the continuous probability density function attributed and considering additional correlations between variables, as described in (Simões et al., 2019a) – see §5.3.2. As the objective is not to obtain the tail of the distributions (i.e. to estimate rare events), the number of required simulations is small and the use of other methods such as Latin Hypercube or importance sampling are not required.

The sampled values are after attributed to the 8 building classes as a function of their probability. For instance, model H-S-S-S-H with a probability of 3.9% is represented by M = 39 models defined by the 39 simulations, whereas model H-S-SH-T-T with a probability of 7.0% is represented by M = 70 models and so forth. This allows to set a group of 1000 building models that comprise the main features that mainly affect the seismic performance of the buildings.

Figure 9 (a) compares the probability density function for the modulus of elasticity of rubble stone masonry, showing a good agreement between the function generated based on the 1000 Monte Carlo simulations and the target function defined by the median value and standard deviation of the reference interval of values. Figure 9 (b) presents, as an example, the probability density function for the drift thresholds that characterize the flexural behaviour of piers at damage levels 3, 4 and 5 (DL3, DL4 and DL5), putting in evidence the higher dispersion for higher damage levels.

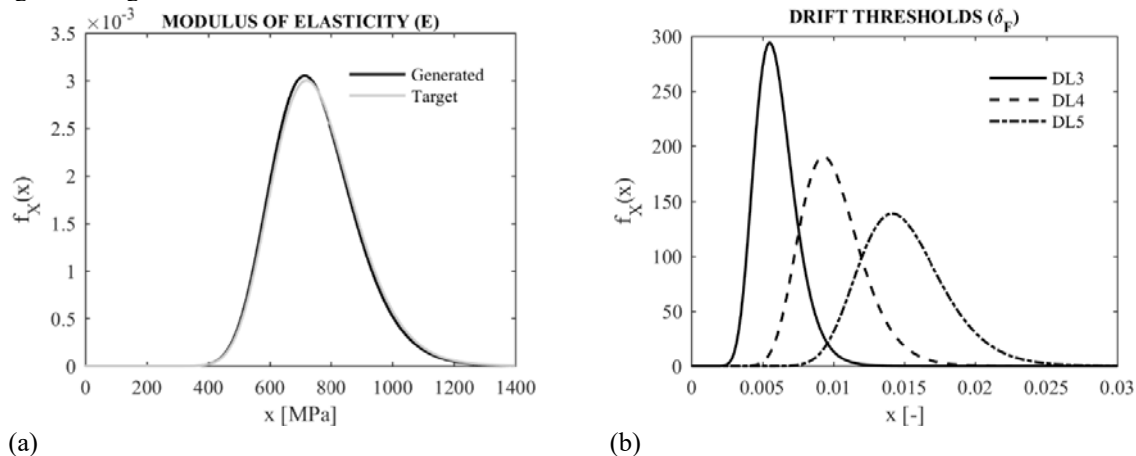(a)   (b)

Figure 9 – Probability density function for: (a) modulus of elasticity of rubble stone masonry and (b) drift thresholds for the flexural behaviour of masonry piers

3.3. Non-linear dynamic analyses to validate the load pattern adopted on the non-linear static (pushover) analyses

The selection of the load distributions to perform non-linear static (pushover) analyses is a critical issue.

Non-linear dynamic analyses are performed with Tremuri program (Lagomarsino et al. 2013) with the objective of checking if the load distributions considered in the non-linear static (pushover) analyses are able to capture the real capacity of the building. To this aim, the same linear piecewise force-deformation constitutive law for masonry panels already used for the pushover analyses (Cattari and Lagomarsino, 2013a) has been adopted since it includes also a specific formulation for describing the hysteretic response differentiated as a function of the

8

main failure modes that can interest the elements. The effectiveness of the program in executing nonlinear dynamic analyses has been recently proven in Cattari et al. (2018).

These analyses are carried out by subjecting the structure to ground-motion acceleration time-histories records compatible with the code seismic action in Lisbon (zone 3) and soil type B (IPQ, 2010). Two types of elastic response spectra are considered with a return period of 475 years (no-collapse requirement) and viscous damping (ξ) of 5%: type 1 – inter-plate earthquake – characterized by a Peak Ground Acceleration (PGA) of 1.50 m/s^2 and soil factor (S) equal to 1.29, and type 2 – intra-plate earthquake – with PGA equal to 1.70 m/s^2 and S equal to 1.27. For each response spectrum type, a set of 30 real ground-motion records were selected with SelEQ tool (Macedo and Castro, 2017). In particular, a preliminary code-based record selection was carried out considering geophysical data (expected magnitude, source-to-site distance, rupture mechanism and soil type) consistent with the two seismic scenarios. The records were after scaled in order that the median of the 30 spectra matched the target response spectrum in the range of periods between $0.2T_1$ and $2T_1$, as established in EC8-1 (IPQ, 2010). T_1 is the fundamental period of the structure in the direction where the record is applied. The average fundamental periods of the 8 building models with median properties were considered in order to comprise all the structural periods (T_{1X}=1.22s and T_{1Y}=0.52s). These values have been confirmed also by the data available on the dynamic identification of real buildings belonging to this typology as based on ambient vibration measurements (see for additional details in Simoes et al. 2019b).

Figure 10 compares the 30 scaled response spectra with the code response spectrum for action type 1 and type 2. Each of the 30 response spectra is defined by the acceleration spectra associated to the geometric mean of the two horizontal components affected by the scale factor.
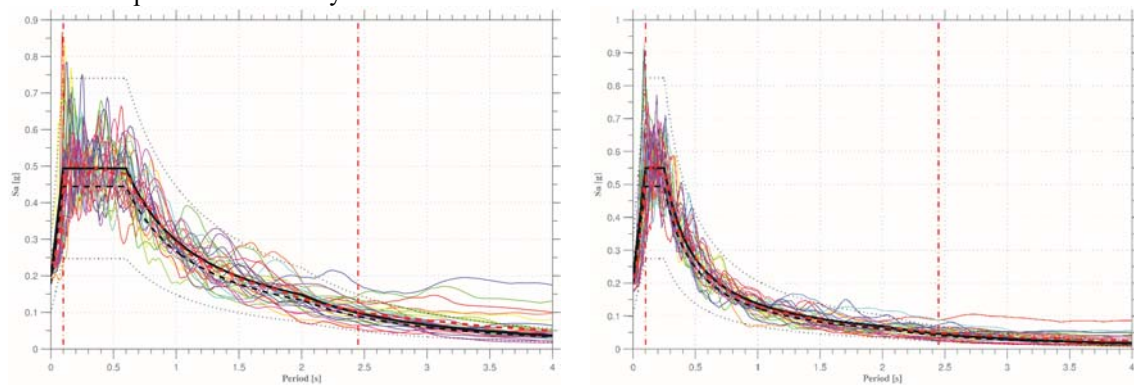

Figure 10 – Comparison of the 30 scaled response spectra with the code response spectrum for action type 1 and type 2

Non-linear dynamic analyses are carried out to the 8 classes of buildings defined by the median properties of the aleatory variables, considering the records compatible with code seismic action type 1 and 2 for Lisbon applied in X and Y directions of the structure. The time-dependent response of the structure is obtained through direct numerical integration of the differential equations of motion of the system, considering both horizontal components of the acceleration spectra acting simultaneously. The effects of viscous damping are considered by adopting the Rayleigh damping formulation and assuming a viscous damping constant and equal to 3%. Here, it is noted that the response of the building in terms of dissipated energy is a composition of inelastic behaviour and viscous damping, Chopra (2001), meaning that higher damping of the response is obtained.

The results obtained from non-linear dynamic analyses (NLDA) and from non-linear static analyses (NLSA) considering the uniform and inverse-triangular load distribution are compared, as exemplified in Figure 11 for building model H-S-S-S-H analysed in Y direction. Since the 30 records were scaled in the range of periods of the structure and not to the same value of peak ground acceleration (PGA), some records produce a quite linear response of the structure while others highlight the strong non-linear response until the collapse of the structure.
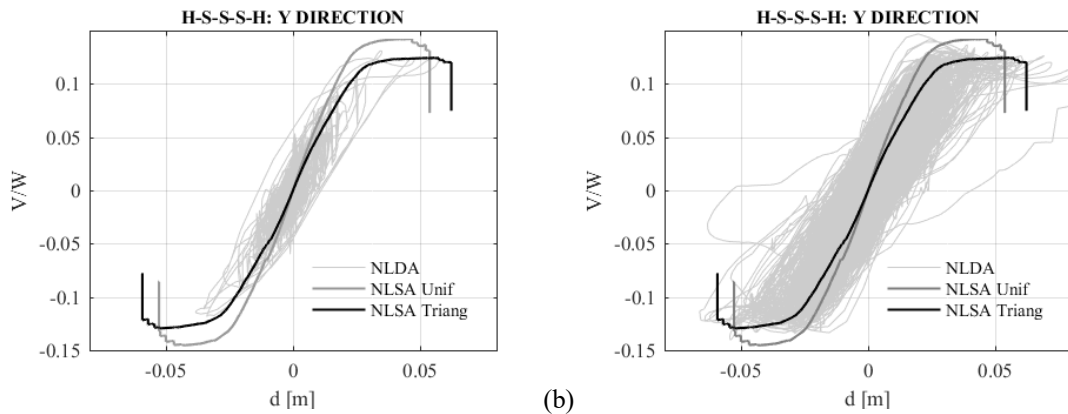
Figure 11 – Model H-S-S-S-H - comparison between NLSA with uniform and inverse-triangular distributions and NLDA by using: (a) a single seismic input and (b) all records compatible with the code action type 1

Despite this general outcome and some uncertainty in the interpretation of results, the analysis record-by-record, as exemplified in Figure 11 (a) reveals that, in general, the non-linear behaviour of the structure may be better characterized by the uniform distribution in the X direction and by the inverse-triangular distribution in the Y direction. That allows to address the choice of this load pattern in the definition of final fragility curves or, at least, two attribute to each force distribution (if uniform or inverse-triangular) a different degree of reliability.

4. Fragility curves for all classes of buildings

4.1. Class of buildings H-S-S-S-H

The procedure adopted for the derivation of fragility functions was illustrated in (Simões et al., 2019a) for the class of buildings H-S-S-S-H. In the following sections, additional information is provided to support the determination of the fragility functions corresponding to the in-plane response (global behaviour, §4.1.1) and out-of-plane response (local behaviour, §4.1.2).

4.1.1. Global behaviour

Non-linear static pushover analyses are carried out to the 39 building models defined by the aleatory variables. The analyses consider the uniform and the inverse-triangular load distributions applied in the X and Y directions negative (-) and positive (+) orientations. Figure 12 presents the plan view of the group of three buildings and the three-dimensional view of the numerical model developed in TREMURI. Figure 13 shows, as an example, the pushover curves obtained by the application of the uniform load distribution in +X and +Y directions. The pushover curves obtained with the model defined by the median properties of the aleatory variables are also included for comparison. As expected, these are not positioned in the middle of the cloud of results.
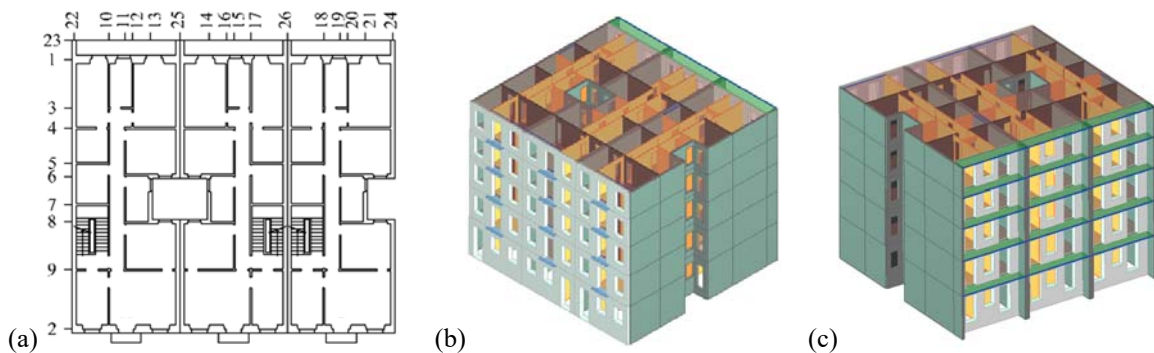

Figure 12 – Group of three buildings: (a) plan view with identification of wall numbering and three-dimensional model in TREMURI (b) street view and (c) rear view
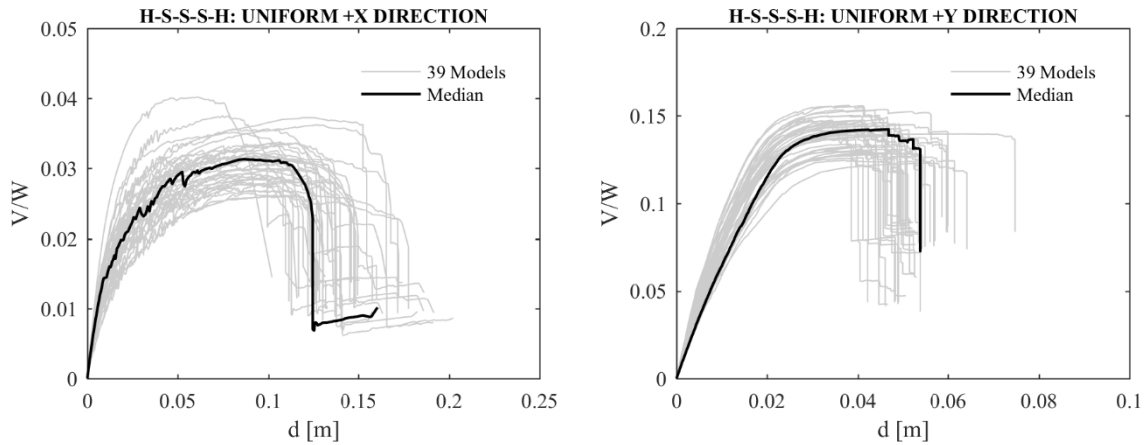
Figure 13 – Pushover curves for H-S-S-S-H considering the uniform load distribution: +X direction (left) and +Y direction (right)

The group of buildings has significantly higher initial stiffness and maximum base shear force in the Y direction than in the X direction. These differences are mainly related with the presence of solid side walls in contrast with the higher number of openings in the X direction. From Figure 14 it is visible that the side walls – 22, 25, 26 and 24 (see Figure 12 (a) for the walls numbering) – have the major contribution to the total base shear in the Y direction, while in the X direction this contribution is distributed between the façade walls – 2 (street) and 1 (rear) – and the interior walls. This is also motivated by the orientation of the timber floors perpendicular to the façade walls, leading to the load distribution between walls in the X direction.

The plan deformation and damage pattern for the maximum displacement of the pushover analysis are shown in Figure 15 and Figure 16, respectively, where the results are obtained by setting all the aleatory variables on their median values. The legend displays the type of failure and damage level in the elements (according to the linear piecewise constitute law proposed by Lagomarsino and Cattari (2015)). The plan deformation of the group of buildings is irregular. In the X direction, wall-2 (street façade) has a uniform deformation, while the remaining walls have a soft-storey mechanism. In the Y direction, the structure has torsional deformation causing a soft-storey mechanism related to the asymmetry of the group and with the position of vertical airshaft on the side of the buildings. Failure occurs due to a flexural behaviour in both directions. Damage in piers is mainly concentrated on the ground floor, while all spandrels reached their maximum strength (≥DL3). In fact, spandrels show a quite weak behaviour since the beginning of the pushover analyses. This is due to the presence of weak lintels and flexible timber floors. The analysis with both load distribution provides similar distribution of damage in the buildings.
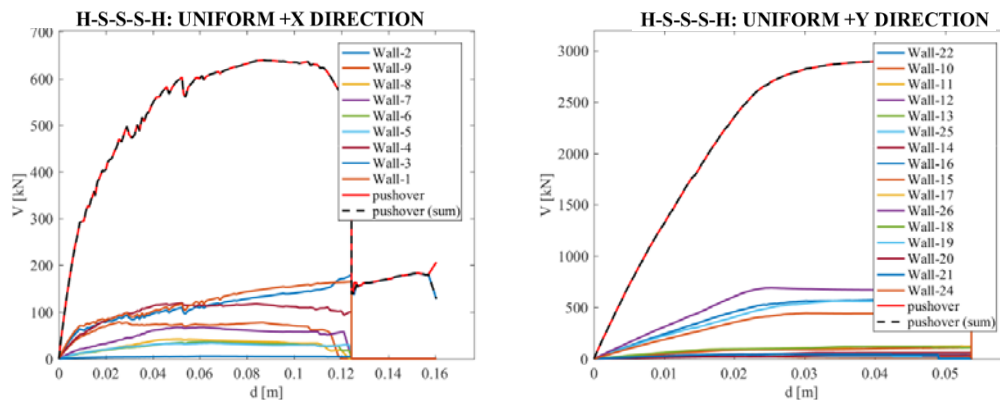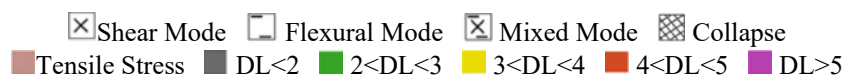

Figure 14 – Pushover curves for H-S-S-S-H configuration setting all the aleatory variables on their median value: Uniform +X direction (left) and +Y direction (right)
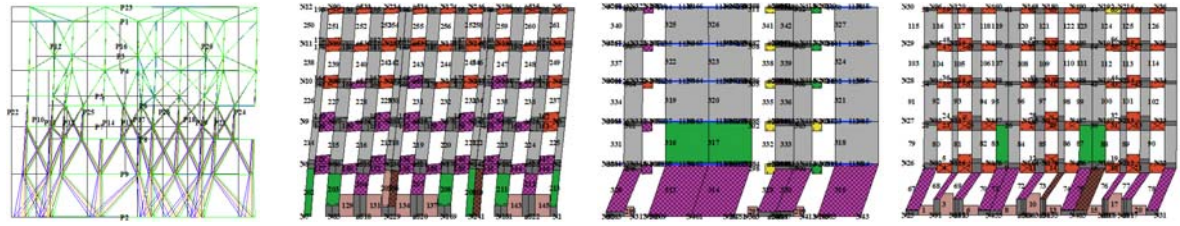
⊠ Shear Mode ▢ Flexural Mode ⊠ Mixed Mode ▨ Collapse
■ Tensile Stress ■ DL<2 ■ 2<DL<3 ■ 3<DL<4 ■ 4<DL<5 ■ DL>5

| Plan deformation | Wall-2 | Wall-4 | Wall-1 |

Figure 15 – Damage in H-S-S-S-H for the maximum displacement: Uniform +X direction

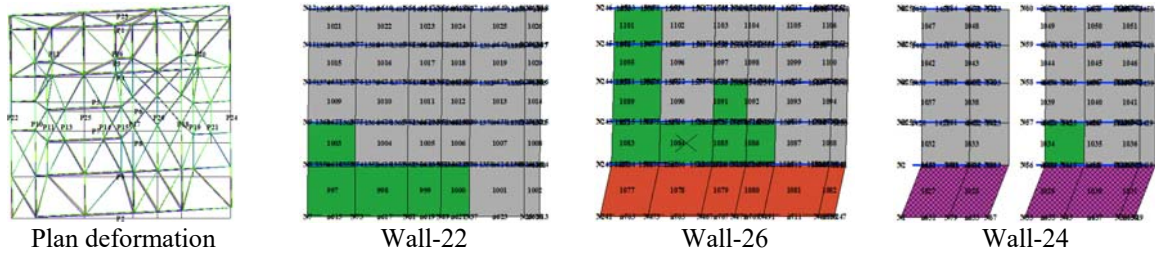| Plan deformation | Wall-22 | Wall-26 | Wall-24 |

Figure 16 – Damage in H-S-S-S-H for the maximum displacement: Uniform +Y direction

The main purpose of performing these non-linear static analyses is to evaluate the capacity of the class of buildings, the variability in the definition of the capacity (β_C) and, with the latter, determine the fragility curves associated for the global behaviour. The intensity measure compatible with PL, IM_{PL}, is obtained from the application of the Capacity-Spectrum Method with overdamped spectrum and without any iterative procedure, as proposed in (Lagomarsino and Cattari, 2015). Two types of seismic input are considered for the assessment (IPQ, 2010): type 1 – inter-plate earthquake – and type 2 – intra-plate earthquake. Figure 17 compares the fragility curves obtained with both seismic actions.

These fragility curves are derived by considering the minimum between the fragility curves obtained in the X and Y directions, as this leads to the most demanding condition for the group of buildings and since it is not possible to predict the main direction of seismic action at priori. On the other hand, it is observed that the most demanding condition is obtained with seismic action type 1 for all PLs, defined by lower values of $PGA_{50\%}$. Finally, it is useful to recall that, as clarified in (Simões et al., 2018), the dispersion related to the global seismic behaviour β_G takes into account both the aleatory variability in the definition of the capacity, β_C, the aleatory uncertainty in the seismic demand, β_D.
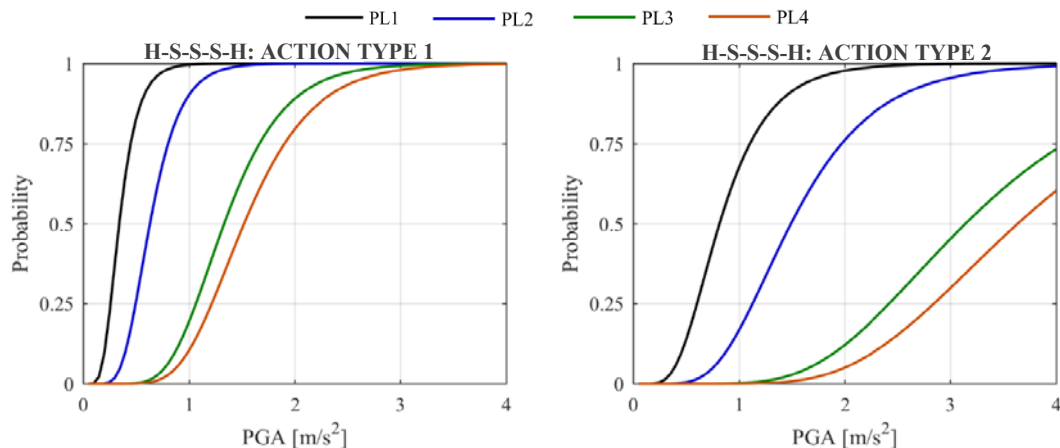

Figure 17 – Fragility functions for H-S-S-S-H global behaviour: seismic action type 1 (left) and type 2 (right)

4.1.2. Local behaviour

Following the discussion in (Simões et al., 2018; see §5.3.1), two possible scenarios were identified for the local seismic behaviour of the buildings related to the response of: 1) the last floor of the building and 2) the parapet. In particular, capacity curves are defined through non-linear kinematic analyses, carried out to local mechanisms identified as the most probable that is (Simões et al., 2018): Mech. 1 – overturning of the central pier; Mech. 2 – flexural mechanism of the central pier; and Mech. 3 – overturning of the parapet. Figure 18 plots the capacity curves obtained from the models set to perform the full factorial analyses and the models defined by the median properties of the aleatory variables.
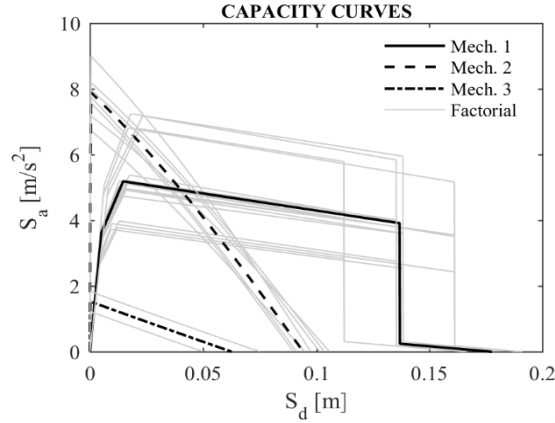
12

Figure 18 – Capacity curves for the local behaviour

The two possible scenarios were assumed as epistemic uncertainties and treated by the logic-tree approach. The fragility curves associated to each scenario are derived taking into account the probability attributed to the different options. Figure 19 provides the resulting fragility curves for both scenarios and compares the curves obtained by considering seismic action type 1 and type 2. As in the global behaviour, it is observed that the most demanding condition for the structure is obtained with seismic action type 1, defined by lower values of $PGA_{50\%}$.
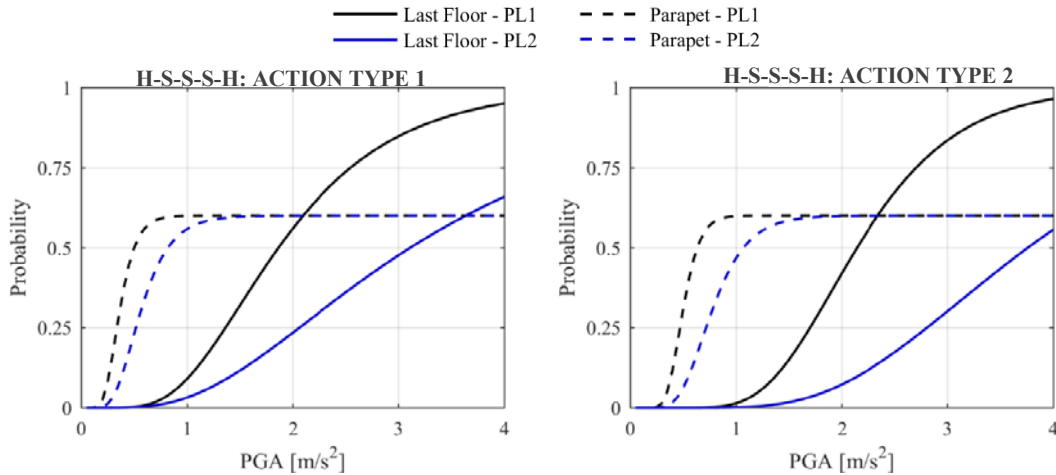

Figure 19 – Fragility functions for H-S-S-S-H local behaviour: seismic action type 1 (left) and type 2 (right)

4.2. Comparison between classes of buildings

This section compares the individual fragility curves for the classes of buildings, after the combination between global and local seismic behaviour, as described in (Simões et al., 2019a; see §6.3). First, the global behaviour in the Y direction of the structure is combined with the local behaviour. The contribution of the local behaviour is limited to the mechanisms involving the last floor of the buildings (first scenario). This is justified because the overturning of the parapets (second scenario) is secondary for the verification of the main structure at a global scale and can be easily prevented by simple strengthening interventions. Second, the minimum between the results obtained in the X and Y directions, the later including the local behaviour, is considered, as this leads to the most demanding condition for the structure.

The parameters that characterize the fragility functions for the different classes of buildings are compared in Figure 20 and Figure 21, respectively, in terms of $PGA_{50\%}$ and total dispersion β, for different PLs. The corresponding values are presented in Table 1 and Table 2, respectively, for seismic action type 1 and type 2. The probability (w_j) of each class of buildings is also indicated. Due to the different contributions, the resulting fragility curves are not a lognormal cumulative distribution function. The dispersion β is determined in an approximated way, considering the values of PGA corresponding to the 84% and 16% percentile of the distribution, according to Equation (1):

$$\beta = \frac{1}{2}\left|\log(PGA_{84\%}) - \log(PGA_{16\%})\right| \tag{1}$$
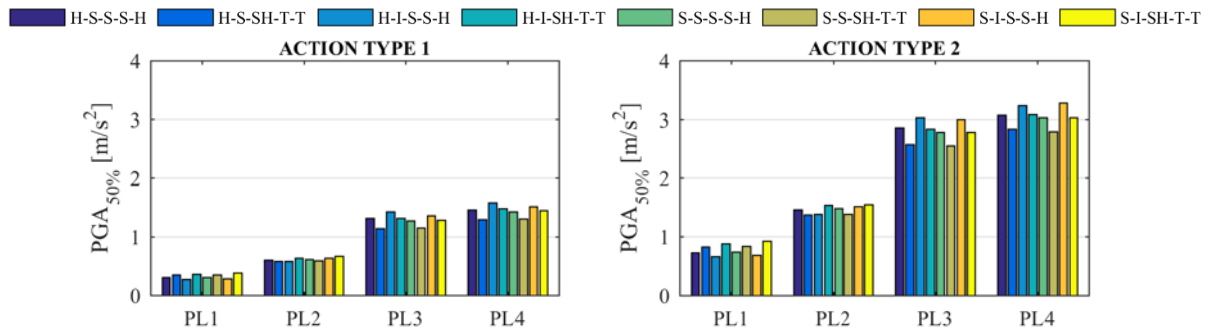
Figure 20 – Median values of PGA for all classes of buildings: seismic action type 1 and type 2
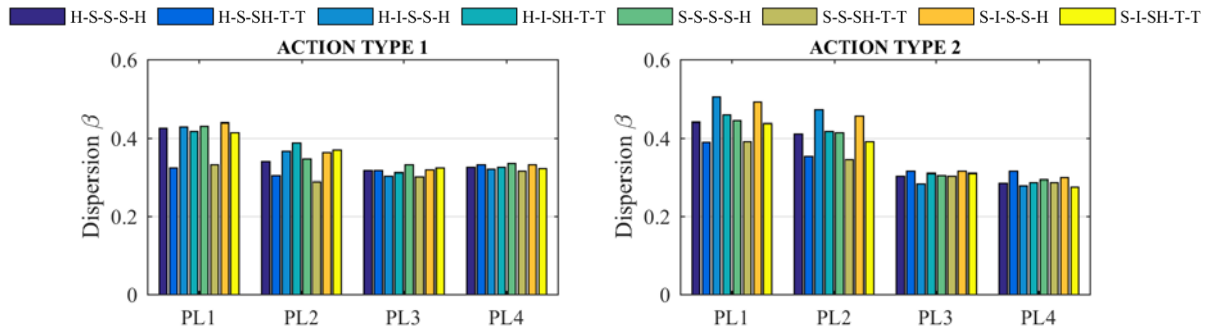

Figure 21 – Dispersion for all classes of buildings: seismic action type 1 and type 2

Table 1 – Fragility curves parameters for all classes of buildings: seismic action type 1

Action Type 1		PL1		PL2		PL3		PL4	
Class of Buildings	w_j	$PGA_{50\%}$ [m/s²]	β	$PGA_{50\%}$ [m/s²]	β	$PGA_{50\%}$ [m/s²]	β	$PGA_{50\%}$ [m/s²]	β
H-S-S-S-H	0.039	0.303	0.426	0.608	0.341	1.326	0.318	1.470	0.326
H-S-SH-T-T	0.070	0.350	0.324	0.588	0.304	1.145	0.317	1.296	0.333
H-I-S-S-H	0.078	0.275	0.430	0.579	0.367	1.428	0.303	1.590	0.320
H-I-SH-T-T	0.143	0.368	0.419	0.643	0.389	1.321	0.313	1.492	0.325
S-S-S-S-H	0.078	0.305	0.431	0.621	0.347	1.276	0.332	1.428	0.335
S-S-SH-T-T	0.143	0.354	0.333	0.592	0.290	1.160	0.300	1.314	0.315
S-I-S-S-H	0.159	0.283	0.440	0.634	0.364	1.365	0.319	1.515	0.332
S-I-SH-T-T	0.290	0.383	0.415	0.674	0.371	1.291	0.324	1.452	0.323

Table 2 – Fragility curves parameters for all classes of buildings: seismic action type 2

Action Type 2		PL1		PL2		PL3		PL4	
Class of Buildings	w_j	$PGA_{50\%}$ [m/s²]	β	$PGA_{50\%}$ [m/s²]	β	$PGA_{50\%}$ [m/s²]	β	$PGA_{50\%}$ [m/s²]	β
H-S-S-S-H	0.039	0.727	0.441	1.460	0.411	2.870	0.302	3.078	0.286
H-S-SH-T-T	0.070	0.826	0.390	1.372	0.354	2.578	0.316	2.845	0.315
H-I-S-S-H	0.078	0.659	0.506	1.388	0.472	3.028	0.284	3.236	0.280
H-I-SH-T-T	0.143	0.884	0.460	1.542	0.419	2.840	0.310	3.085	0.287
S-S-S-S-H	0.078	0.732	0.445	1.489	0.415	2.793	0.304	3.030	0.295
S-S-SH-T-T	0.143	0.836	0.392	1.387	0.345	2.560	0.302	2.796	0.288
S-I-S-S-H	0.159	0.680	0.493	1.520	0.456	2.999	0.316	3.285	0.299
S-I-SH-T-T	0.290	0.921	0.438	1.556	0.392	2.792	0.310	3.030	0.276

Comparing the 8 classes of buildings, it may be concluded that, in general, lower values of PGA are obtained for classes of buildings:

a) with timber walls (#-#-SH-T-T) in comparison with ones without such walls (#-#-S-S-H);

b) with shared side walls (#-S-#-#-#) in comparison with independent side walls (#-I-#-#-#);

c) with ground floor used as shop (S-#-#-#-#) in comparison with the use as house (H-#-#-#-#);

d) and for seismic action type 1 in comparison with type 2.

This is particular true for the higher performance levels, PL3 and PL4. Figure 22 exemplifies some of these features. It is also observed that, in general, higher dispersion is obtained for PL1 and PL2 while the dispersion for PL3 and PL4 is similar across the different classes of buildings. It seems consistent with the fact that the initial response is more sensitivity to the different structural features which characterize each configuration but at the end the final global mechanism occurred is almost the same (that is a soft-story mechanism). Moreover, it is worth observing that a reliable determination of performance levels associated to a slight damage is typically a difficult task, justifying in part the results obtained.

Moreover, it was also concluded that the final dispersion is mainly due to the contribution of the dispersion in the seismic demand (β_D), due to the large variability of possible ground-motion records. This result is confirmed by many other literature works, as for example recently testified by results presented in (RINTC, 2018) as a function of different structural typologies (masonry, reinforced concrete, steel and precast reinforced concrete).
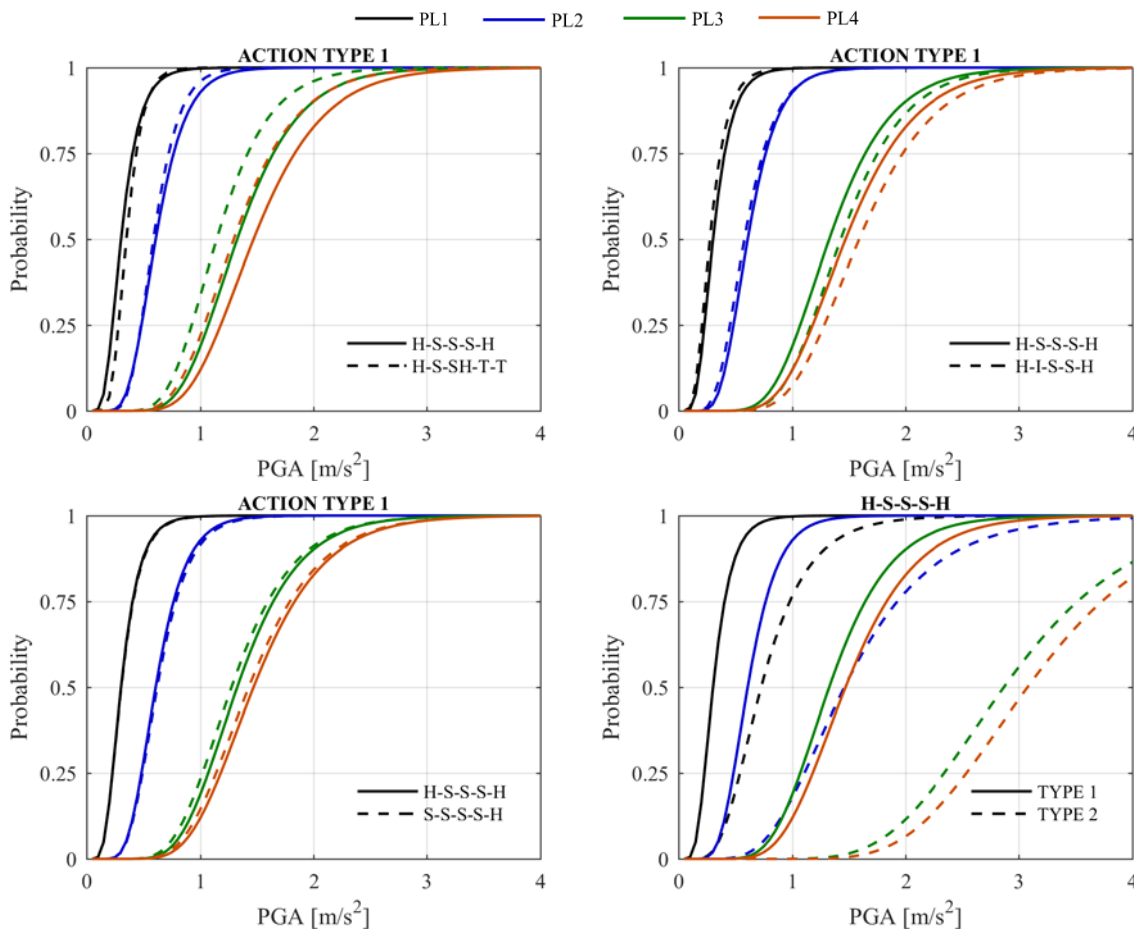

Figure 22 – Comparison of fragility curves between H-S-S-S-H and: (a) H-S-SH-T-T, (b) H-I-S-S-H, (c) H-S-S-S and (d) action type 1 and type 2

5. Fragility curves for the typical URM tall buildings

This section addresses the derivation of the fragility functions for the typical URM tall buildings by considering the contribution of the different classes of buildings identified. These fragility curves take into account the different sources of uncertainties that influence the seismic performance of the buildings, providing the overall assessment of the seismic vulnerability of this class of buildings at territorial scale.

The final fragility curves are obtained by adding the fragility curves of the different classes of building as a function of their probability (w_j). This is defined in an approximated way by the application of Equation (2) and Equation (3):

$$PGA_{50\%} = \sum_{j=1}^{8} w_j PGA_{50\%,j} \tag{2}$$

$$\beta = \sqrt{\sum_{j=1}^{8} w_j \beta_j^2} \tag{3}$$

Table 3 summarizes the parameters for the fragility functions considering the global seismic behaviour of the typology and Figure 23 plots the corresponding functions for seismic action type 1 and type 2.

Table 3 – Resulting parameters of fragility curves for the typical tall URM buildings

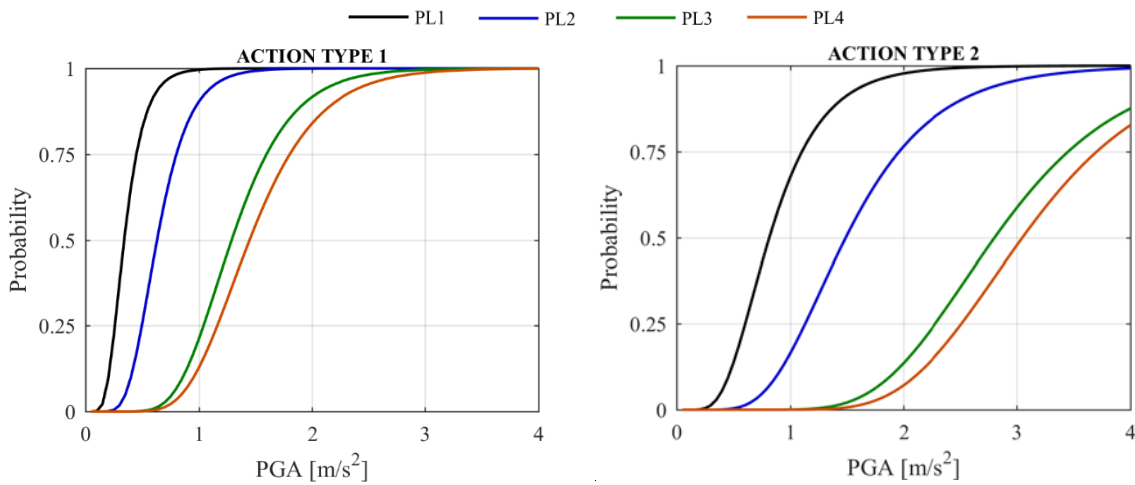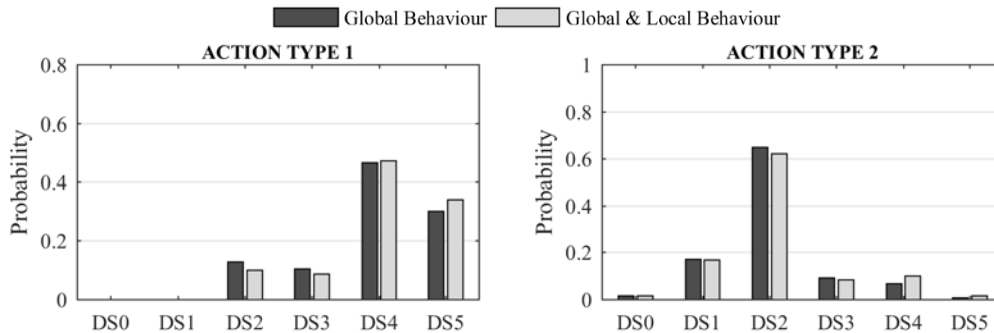| PL	Action Type 1		Action Type 2	
	$PGA_{50\%}$ [m/s²]	β	$PGA_{50\%}$ [m/s²]	β
1	0.341	0.406	0.816	0.447
2	0.631	0.354	1.489	0.407
3	1.289	0.317	2.805	0.308
4	1.447	0.325	3.050	0.288

Figure 23 – Fragility functions for the typical tall URM buildings: seismic action type 1 (left) and type 2 (right)

The discrete probability associated with the different damage states is determined following the procedure presented in (Simões et al., 2019a; see §2). The code seismic actions for Lisbon (IPQ, 2010) for a return period of 475 years are considered for the estimation of the damage distribution: type 1 (PGA at surface, i.e. PGA*S = 1.94 m/s²) and type 2 (PGA*S = 2.16 m/s²). Figure 24 shows the corresponding probability damage distribution. The probability damage distribution obtained considering only the global seismic behaviour of the buildings is also included for comparison. As expected, the contribution of the local seismic behaviour increased the final vulnerability for the higher damage states.

Distribution of damage		DS0	DS1	DS2	DS3	DS4	DS5
Action Type 1 PGA*S = 1.94 m/s²	Global Behaviour	0.000	0.001	0.128	0.104	0.467	0.301
	Global & Local Behaviour	0.000	0.001	0.099	0.085	0.474	0.341
Action Type 2	Global Behaviour	0.015	0.171	0.649	0.089	0.066	0.009

PGA*S = 2.16 m/s^2	Global & Local Behaviour	0.015	0.167	0.622	0.082	0.099	0.015

Figure 24 – Distribution of damage for the URM buildings of type I for seismic action type 1 (PGA*S=1.94 m/s^2) and type 2 (PGA*S=2.16 m/s^2)

The fragility functions derived highlight the high seismic vulnerability of the buildings, particularly for seismic action type 1. It is estimated that there is about 47% probability of having very heavy damage (DS4) and about 34% probability of collapse (DS5). These results are in line with previous studies about these buildings, as discussed in detail in (Simões, 2018). Nevertheless, the number of fragility functions available in the literature addressed to the URM buildings in Lisbon is scarce. Reference for example to the works developed about the "Pombalino" buildings constructed after the 1755 earthquake (Lopes et al., 2014; Meireles et al., 2014), about the "gaioleiro" buildings (Simões et al., 2014; Simões et al., 2015) and about the mixed masonry-RC structure (Lamego et al., 2017; Milošević, 2018). In Simões et al. (2015) a comparison of the fragility curves obtained for the three typologies of buildings is presented.

These outcomes, put in evidence the high seismic vulnerability of these tall URM buildings and the urgent need to reduce potential losses due to future earthquakes. In this regard, it was verified that concerning the local out-of-plane response, the buildings are particularly vulnerable to the overturning of the central piers from the last floor and of the parapets. In fact, the probability distribution of damage for the code seismic action for Lisbon and for a return period of 475 years indicates the sure collapse of the parapets for both types of action. A possible intervention is to fix this non-structural element at its base or to the roof structure by the application of steel tie-rods. Concerning the global response, the main criticality of the buildings in the direction of the side walls, is related to the insufficient capacity in terms of ductility more than overall strength, while in the direction of the façade walls the opposite occurs. Thus, the improvement of the connection between perpendicular walls and between walls and horizontal diaphragms, as well as the increase of the in-plane stiffness of the later ones, should be considered as a first approach to improve the global response and reduce the seismic vulnerability of the buildings. A second approach would be to increase the in-plane capacity of the masonry walls through reinforced plasters or by the introduction of new shear walls.

6. Final Remarks

The article presents the overall seismic vulnerability assessment of a class of tall URM buildings supported on the definition of different classes of buildings. Thus, the features that mostly affect the seismic performance are identified based on the available information at territorial scale. These features are considered as epistemic uncertainties (related to the incomplete knowledge) and are treated by the logic-tree approach. This aims to define different classes representative of the URM buildings constructed in Lisbon in the early 20th century. For each class of buildings, fragility curves are generated taking into account both the in-plane plane and out-of-plane seismic response, following the procedure proposed in a companion article (Simões et al., 2019a). The fragility curves obtained for the global and local behaviour are after combined in order to define fragility curves representative of the class of tall URM buildings.

Results for a seismic event, as defined in the earthquake-resistant code for Lisbon and for a return period of 475 years, indicate that the typical buildings constructed in the early 20th century in Lisbon and studied in this work, have about 50% probability of having heavy damage and about 30% probability of collapse. Here, it is important to refer that these results represent the upper line of the expected distribution of damage, taking into account that: 1) the worst case scenario was considered in the main steps of the methodology and, 2) the recommendation given by the Portuguese National Annex to the EC8-3 (IPQ, 2017) to reduce of the reference peak ground acceleration for the assessment of existing buildings was disregarded. Nevertheless, these results put in evidence the high seismic vulnerability of these buildings and the urgent need for the structural intervention and for the design of retrofitting measures to reduce potential losses due to future earthquakes. The fragility curves obtained for this work for URM buildings are compared with the fragility curves derived in other studies in Simões et al. (2019b). The article also addresses strategies to improve the procedure for the derivation of fragility functions. Preliminary non-linear static analyses indicated that some classes of buildings present a similar global response allowing to reduce the number of classes to be considered in the final and detailed assessment. Non-linear dynamic analyses with time integration are performed with the objective of verifying if the load distributions considered in the non-linear static analyses are able to capture the global behaviour of the buildings. It is concluded that both uniform (in X direction) and inverse-triangular load (in Y direction) distributions should be considered. Although, this result is specific of the building classes examined the procedure proposed is general and could be efficiently applied also to another structural context.

References

Appleton JG. (2005) Reabilitação de Edifícios "Gaioleiros." 1st ed. Lisboa: Edições Orion (In Portuguese).

Cattari S, Camilletti D, Lagomarsino S, Bracchi S, Rota M, Penna A (2018) Masonry Italian Code-Conforming Buildings. Part 2: Nonlinear Modelling and Time-History Analysis, Journal of Earthquake Engineering, Taylor and Francis, 22(sup2), 2010-2040, DOI: 10.1080/13632469.2018.1541030.

Chopra, A.K. (2016). Dynamics of structures: theory and applications to earthquake engineering. 5th ed. Prentice Hall.

IPQ (2017) Eurocódigo 8 – Projeto de estruturas para resistência aos sismos Parte 3: Avaliação e reabilitação de edifícios, NP EN 1998-3:2017. Instituto Português Da Qualidade (IPQ). Caparica (In Portuguese).

IPQ. (2010) Eurocódigo 8 - Projecto de estruturas para resistência aos sismos. Parte 1: Regras gerais, acções sísmicas e regras para edifícios, NP EN 1998-1:2010. Instituto Português Da Qualidade (IPQ). Caparica (In Portuguese).

Lagomarsino S, Cattari S. (2015) Seismic Performance of Historical Masonry Structures Through Pushover and Nonlinear Dynamic Analyses. In: Ansal A, editor. Perspectives on European Earthquake Engineering and Seismology, Geotechnical, Geological and Earthquake Engineering, 39, vol. 39, Springer International Publishing; 2015. DOI: 10.1007/978-3-319-16964-4.

Lagomarsino S, Penna A, Galasco A, Cattari S (2013) TREMURI program: An equivalent frame model for the nonlinear seismic analysis of masonry buildings. Engineering Structures 2013; 56: 1787–1799. DOI: 10.1016/j.engstruct.2013.08.002.

Lamego P, Lourenço PB, Sousa ML, Marques R (2017) Seismic vulnerability and risk analysis of the old building stock at urban scale: application to a neighbourhood in Lisbon. Bulletin of Earthquake Engineering 2017; 15(7): 2901–2937. DOI: 10.1007/s10518-016-0072-8.

Lopes M, Meireles H, Cattari S, Bento R, Lagomarsino S (2014) Pombalino Constructions: Description and Seismic Assessment. In: Costa A, Guedes JM, Varum H, editors. Structural Rehabilitation of Old Buildings, Building Pathology and Rehabilitation, 2. 1st ed., Springer Berlin Heidelberg; 2014. DOI: 10.1007/978-3-642-39686-1.

Macedo L, Castro JM (2017) SelEQ: An advanced ground motion record selection and scaling framework. Advances in Engineering Software 2017; 114: 32–47. DOI: 10.1016/j.advengsoft.2017.05.005.

Meireles H, Bento R, Cattari S, Lagomarsino S (2014) Seismic assessment and retrofitting of Pombalino buildings by pushover analyses. Earthquake and Structures 2014; 7(1): 57–82. DOI: 10.12989/eas.2014.7.1.057.

Milošević J, Cattari S, Bento R (2018) Sensitivity analyses of seismic performance of ancient mixed masonry-RC buildings in Lisbon International Journal of Masonry Research and Innovation, Inderscience Publishers, Vol. 3, Nº 2, 108-154.

RGEUL (1930) Regulamento Geral das Edificações Urbanas em Lisboa (RGEUL). Postura Da Câmara Municipal de Lisboa de 28/08/1930. Lisboa (In Portuguese).

RINTC Workgroup. Results of the 2015-2017 Implicit seismic risk of code- conforming structures in Italy (RINTC) project. Naples: 2018.

Rubinstein RY. (2011) Simulation and the Monte Carlo Method. John Wiley & Sons, Inc..

Simões A, Bento R, Cattari S, Lagomarsino S (2014) Seismic Assessment of "Gaioleiro" buildings in Lisbon. Proceedings of the 9th International Masonry Conference, Guimarães.

Simões A, Bento R, Lagomarsino S, Lourenço PB. (2016) Simplified evaluation of seismic vulnerability of early 20th century masonry buildings in Lisbon. Proceedings of the 10th International Conference on Structural Analysis of Historical Constructions, Leuven.

Simões A, Milošević J, Meireles H, Bento R, Cattari S, Lagomarsino S (2015) Fragility curves for old masonry building types in Lisbon. Bulletin of Earthquake Engineering 2015; 13(10): 3083–3105. DOI: 10.1007/s10518-015-9750-1.

Simões A. (2018) Evaluation of the seismic vulnerability of the unreinforced masonry buildings constructed in the transition between the 19th and 20th centuries in Lisbon, Portugal. PhD Thesis. Instituto Superior Técnico, Universidade de Lisboa. Lisboa.

Simões AG, Bento R, Lagomarsino S, Cattari S, Lourenço PB. (2019a) Fragility functions for tall URM buildings around early 20th century in Lisbon. Part 1: method description and application to a case study. International Journal of Architectural Heritage (in Revision).

Simões AG, Bento R, Lagomarsino S, Cattari S, Lourenço PB. (2019b) "Seismic assessment of nineteenth and twentieth centuries URM buildings in Lisbon: structural features and derivation of fragility curves", Bulletin of Earthquake Engineering, Elsevier, A. Ansal editor, Springer. DOI: 10.1007/s10518-019-00618-z

Simões AG, Bento R, Lagomarsino S, Lourenço PB. (2018) The seismic assessment of masonry buildings between the 19th and 20th centuries in Lisbon - Evaluation of uncertainties. Proceedings of the 10th International Masonry Conference, Milan